Systematic studies of nuclei around mass 130 in the pair-truncated shell model

N. Yoshinaga[1,*] and K. Higashiyama[1,2,†]
[1]*Department of Physics, Saitama University, Saitama City 338-8570, Japan*
[2]*RIKEN (The Institute of Physical and Chemical Research), Wako, Saitama 351-0198, Japan*
(Received 13 February 2004; published 19 May 2004)

Systematic studies are carried out for Xe, Ba, Ce, and Nd isotopes within the framework of the pair-truncated shell model where the collective nucleon pairs with angular momenta zero (S) and two (D) are assumed to be the building blocks for even-even nuclei. An additional unpaired nucleon is added to the even-even core for a description of odd-mass nuclei. It is found that energy spectra of the low-lying states are nicely reproduced along with intraband and interband $E2$ transitions, which simulate the typical features of the O(6) limit of the interacting boson model.

DOI: 10.1103/PhysRevC.69.054309 PACS number(s): 21.10.Re, 21.60.Cs, 21.60.Ev, 27.60.+j

I. INTRODUCTION

Nuclei around mass 130 have many interesting features such as high-spin isomers, backbending phenomena, even-odd energy staggering of quasi-γ bands caused by a soft triaxial deformation, and features recently referred to as "chiral bands." Moreover, beta decays in this region provide us with necessary information for predicting the abundance of nuclei in the environment of supernova explosions. These nuclei belong to a typical transitional region between spherical and deformed shapes. The even-even nuclei in this region seem to be soft with regard to the γ deformation with an almost maximum effective triaxiality of $\gamma \sim 30°$ [1,2]. Since they are neither vibrational nor rotational, it is very difficult to treat them in terms of conventional mean field theories.

The low-lying states, showing a rich collective structure in this region, were investigated extensively in terms of various models, such as the interacting boson model (IBM) [2–13], the fermion dynamical symmetry model (FDSM) [14–16], the pair-truncated shell model (PTSM) [17–22], and the nucleon-pair shell model [23–26]. Some phenomenological IBM calculations as in Ref. [6] show that the excitation spectra of the even-even nuclei in the Xe-Ba mass region can be well approximated by the O(6) dynamical symmetry of the IBM. However, as suggested by Ref. [13], the nuclei around this region might have an intermediate structure between the U(5) and SU(3) limits. The present scheme provides a theoretical method to settle the differences between these different IBM approaches, the O(6) approach and the U(5)-SU(3) one coming from the degree of γ softness since the microscopic approach truncated in the S and D pairs is directly connected to the microscopic foundation of the IBM.

Odd-mass nuclei in mass $A \sim 130$ region often show complicated level schemes, which arise from the coupling of collective and single-particle degrees of freedom. One of the approaches first used to explain the experimental properties was the particle triaxial core model [27–29]. Its application to the Ba isotopes indicated the importance of triaxial deformation in this region. A widely used tool for describing the odd-mass nuclei is the interacting boson-fermion model (IBFM) [30]. The simplest version of the IBFM (IBFM-1) was applied to negative and positive parity states of the odd-mass Xe and Ba isotopes, and the complicated level schemes and electromagnetic properties were well reproduced [31]. Using different sets of single-particle orbitals, similar calculations were carried out for the negative parity states of the nuclei $^{123-133}$Ba and $^{117-131}$Xe [33], and for the positive parity states of the nuclei $^{121-133}$Ba and $^{121-131}$Xe [32], and for both positive and negative parity states of the nuclei $^{121-131}$Ba [34]. Similarly, the IBFM-2 calculations were performed for the odd-mass Xe and Cs isotopes [35,36], and Ba and La isotopes [37]. These approaches could also qualitatively describe the evolution of the collective motions and excitations of single-particle degrees of freedom in this mass region. Recently, the systematic study in the $A \sim 130$ nuclei was performed in terms of the FDSM [16], and energy spectra of positive parity states were well reproduced. In order to investigate the validity of a microscopic derivation of the IBM and IBFM Hamiltonian, Yoshinaga *et al.* calculated the energy levels of the singly closed even-even and odd-mass nuclei in $A \sim 130$ region in terms of the shell model, the IBM and IBFM, and the PTSM [21]. It was shown that the PTSM and IBFM calculations quantitatively reproduce the shell model results for the odd-mass nuclei, and the truncation scheme for the SD pair plus one-particle space provides an effective and minimal shell-model space.

In this paper we first construct many-body states for even-even nuclei within the framework of the SD version of the PTSM and carry out an extensive study to search for the best effective interactions around mass $A=130$. The PTSM is a model beyond mean field theories and has the feature that the model conserves particle numbers and angular momenta of the states. In order to find a best set of interactions within the PTSM, the χ^2 fitting is carried out for the low-lying states of even-even Xe, Ba, and Ce nuclei to determine the strengths of the pairing plus quadrupole type interactions. The strengths of the interactions are assumed to be smooth functions of the proton number Z and the neutron number N. The obtained interactions are applied to both Nd isotopes and to odd-mass nuclei without any further change.

*Electronic address: yoshinaga@phy.saitama-u.ac.jp
†Electronic address: higashi@phy.saitama-u.ac.jp

The paper is organized as follows. In Sec. II, the framework of the PTSM and its effective interaction in the model space are presented. In Sec. III A the PTSM calculations are carried out for Xe, Ba, Ce, and Nd isotopes with mass $A \sim 130$, where the effective interactions are smoothly changed as functions of valence particles. In Sec. III B we extend the PTSM for an application to odd-mass nuclei, and carry out calculations for Xe, Ba, and Ce isotopes. Principal results are summarized in Sec. IV.

II. FRAMEWORK OF THE PTSM AND ITS *SD*-PAIR TRUNCATION

In the shell model calculation, the number of configurations increases exponentially with the number of particles, and the treatment becomes soon infeasible for the present computers. Therefore, if the number of valence nucleons is large, a treatment by the full-fledged shell model has to be abandoned, and a truncation of the space or some sort of approximation is required.

In the first stage of the PTSM, we truncate the collective subspace to the space which is constructed only in terms of collective S and D pairs. These pairs, as building blocks of the model, are defined in terms of pair-creation operators as

$$S^\dagger = \sum_j \alpha_j A_0^{\dagger(0)}(jj), \tag{1}$$

$$D_M^\dagger = \sum_{j_1 j_2} \beta_{j_1 j_2} A_M^{\dagger(2)}(j_1 j_2), \tag{2}$$

where the structure coefficients α and β are determined by variation in the present approach for each nucleus. Here the creation operator of a pair of nucleons with total spin J and projection M is defined as follows:

$$A_M^{\dagger(J)}(j_1 j_2) = [c_{j_1}^\dagger c_{j_2}^\dagger]_M^{(J)}, \tag{3}$$

where $c_j^\dagger$ represents a single-particle creation operator in orbital j for protons and a single-hole creation operator for neutrons. In this atomic mass region we treat neutrons as holes and protons as particles so that $N=82$ and $Z=50$ become the nearest closed shells. These pairs are constructed in each neutron or proton space separately.

The structure coefficients α and β are determined so as to maximize the collectivity of the S and D pairs. More explicitly, the structure of the collective S pair is determined by variation for an n-pair state $|S^n\rangle = (S^\dagger)^n|-\rangle$,

$$\delta\langle S^n|H|S^n\rangle = 0, \tag{4}$$

which is considered as a number conserved BCS equation in each neutron or proton space. Here, H is an interaction among like nucleons. In the second step, with use of the S-pair obtained above, the structure of the collective D pair is determined by

$$\delta\langle S^{n-1}D|H|S^{n-1}D\rangle = 0. \tag{5}$$

Using the collective S and D pairs thus obtained, a many-body state is constructed as

$$|S^{n_s}D^{n_d}J\eta\rangle = (S^\dagger)^{n_s}(D^\dagger)^{n_d}|-\rangle, \tag{6}$$

where J indicates the total spin of the many-body state, η is a quantum number which is necessary to uniquely specify the state, and n_s+n_d represents the number of valence pairs for a specific nucleus. Here angular momentum coupling is carried out exactly, but for simplicity it is not denoted explicitly.

In order to describe open-shell nuclei, we use the above states in both neutron and proton spaces to couple them to the state with total angular momentum J. The total state is expressed as follows:

$$|\Phi(J\eta)\rangle = [|S_\nu^{\bar{n}_s}D_\nu^{\bar{n}_d}J_\nu\eta_\nu\rangle \otimes |S_\pi^{n_s}D_\pi^{n_d}J_\pi\eta_\pi\rangle]^{(J)}, \tag{7}$$

where $\bar{N}_\nu = 2(\bar{n}_s+\bar{n}_d)$ and $N_\pi = 2(n_s+n_d)$ are numbers of valence neutron-holes and valence proton-particles, respectively.

As an effective interaction, we employ the monopole and quadrupole pairing plus quadrupole-quadrupole interaction ($P+QQ$). The shell model Hamiltonian is written as

$$H = H_\nu + H_\pi + H_{\nu\pi}, \tag{8}$$

where H_ν, H_π, and $H_{\nu\pi}$ represent the neutron interaction, the proton interaction, and the neutron-proton interaction, respectively. The interaction among like nucleons H_τ ($\tau=\nu$ or π) consists of spherical single-particle energies, monopole-pairing (MP) interaction, quadrupole-pairing (QP) interaction, and quadrupole-quadrupole (QQ) interaction, i.e.,

$$H_\tau = \sum_{jm} \varepsilon_{j\tau} c_{jm\tau}^\dagger c_{jm\tau} - G_{0\tau} P_\tau^{\dagger(0)} P_\tau^{(0)} - G_{2\tau} P_\tau^{\dagger(2)} \cdot \tilde{P}_\tau^{(2)} - \kappa_\tau :Q_\tau \cdot Q_\tau:, \tag{9}$$

where :: denotes normal ordering. Here the monopole-pairing operator $P_\tau^{\dagger(0)}$, the quadrupole-pairing operators $P_{M\tau}^{\dagger(2)}$, $\tilde{P}_{M\tau}^{(2)}$ and the quadrupole operator $Q_{M\tau}$ are defined as

$$P_\tau^{\dagger(0)} = \sum_j \frac{\sqrt{2j+1}}{2} A_{0\tau}^{\dagger(0)}(jj), \tag{10}$$

$$P_{M\tau}^{\dagger(2)} = \sum_{j_1 j_2} Q_{j_1 j_2} A_{M\tau}^{\dagger(2)}(j_1 j_2), \tag{11}$$

$$\tilde{P}_{M\tau}^{(2)} = (-)^M P_{-M\tau}^{(2)}, \tag{12}$$

$$Q_{M\tau} = \sum_{j_1 j_2} Q_{j_1 j_2} [c_{j_1\tau}^\dagger \tilde{c}_{j_2\tau}]_M^{(2)}, \quad (\tilde{c}_{jm\tau} = (-1)^{j-m} c_{j-m\tau}), \tag{13}$$

$$Q_{j_1 j_2} = -\frac{\langle j_1 \| r^2 Y^{(2)} \| j_2 \rangle}{\sqrt{5}}, \tag{14}$$

where $A_{M\tau}^{\dagger(J)}(j_1 j_2)$ stands for the creation operator of a pair of nucleons given by Eq. (3). We assume that the interaction between neutrons and protons $H_{\nu\pi}$ is just given by the QQ interaction,

TABLE I. Adopted single-particle energies for neutron holes and proton particles, which are extracted from experiment [38–40] (in MeV).

j	$2s_{1/2}$	$0h_{11/2}$	$1d_{3/2}$	$1d_{5/2}$	$0g_{7/2}$
ε_ν	0.332	0.242	0.000	1.655	2.434
ε_π	2.990	2.793	2.708	0.962	0.000

$$H_{\nu\pi} = -\kappa_{\nu\pi} Q_\nu \cdot Q_\pi. \tag{15}$$

The harmonic oscillator basis states with the oscillator parameter $b=\sqrt{\hbar/M\omega}$ are employed for the single-particle basis states.

III. NUMERICAL INVESTIGATION

A. Even-even nuclei

In our scheme Xe, Ba, Ce, and Nd isotopes are treated as systems of several valence proton particles and neutron holes coupled to the doubly closed ^{132}Sn core. Since the valence neutron holes (proton particles) occupy the $0g_{7/2}$, $1d_{5/2}$, $1d_{3/2}$, $0h_{11/2}$, and $2s_{1/2}$ orbitals, we take into account the $50 \leqslant N(Z) \leqslant 82$ configuration space for neutrons (protons), where valence neutrons (protons) are treated as holes (particles). The adopted single-particle energies, listed in Table I, are extracted from experimental excitation energies in Refs. [38–40].

To determine the strengths of the interactions we follow the following steps. First, several sets of candidates for effective interactions are searched to get smaller values of the following χ^2 values:

$$\chi^2 = \sum W(J_i^\pi)[E_{expt.}(J_i^\pi) - E_{th.}(J_i^\pi)]^2, \tag{16}$$

where $W(J_i^\pi)$ is a weight function for the ith state with spin J and parity π, and $E_{expt.}(J_i^\pi)$, experimental energies and $E_{th.}(J_i^\pi)$, theoretically predicted energies by the PTSM. As for the fitting energy levels, we take low-lying states of the even-even nuclei, $^{128-132}$Xe, $^{130-134}$Ba, and $^{132-136}$Ce. Here we exclude Nd isotopes since it is quite time consuming to calculate them. We take $W(J_i^\pi)=0$ for those levels which are not experimentally confirmed. The assumed values of weight functions are listed in Table II. Next, we apply each set of interactions to the nuclei ^{126}Xe, ^{128}Ba, ^{130}Ce, and $^{132-138}$Nd, and take the best set of effective interactions to describe these nuclei.

The strengths of the effective interactions are assumed to be smoothly changed as functions of the numbers of valence particles. The determined functional dependences are as follows (G_0 of MP interaction in unit of MeV, and G_2 of QP interaction and κ of QQ interaction, both in unit of MeV$/b^4$):

$$G_{0\nu} = 0.160 - 0.010\ \overline{N}_\nu,$$

$$G_{2\nu} = 0.017 + 0.0005\ N_\pi,$$

$$\kappa_\nu = 0.075 - 0.0015\ N_\pi,$$

$$G_{0\pi} = 0.200 - 0.010\ \overline{N}_\nu - 0.005\ N_\pi,$$

$$G_{2\pi} = 0.010 + 0.001\ N_\pi,$$

$$\kappa_\pi = 0.014 + 0.006\ N_\pi,$$

$$\kappa_{\nu\pi} = -0.044 - 0.002\ \overline{N}_\nu, \tag{17}$$

where $\overline{N}_\nu$ indicates the number of valence neutron holes and N_π, the number of valence proton particles. This choice of the strengths of interactions gives χ^2 value =0.442 for 104 levels of even-even nuclei, $^{126-132}$Xe, $^{128-134}$Ba, $^{130-136}$Ce, and $^{132-138}$Nd.

TABLE II. Adopted weight functions $W(J_i^\pi)$ for χ^2 fitting (in MeV^{-2}).

$\overline{N}_\nu+N_\pi$	2_1^+	4_1^+	6_1^+	2_2^+	3_1^+	4_2^+	5_1^+
8	1.00	1.00	0.16	1.00	0.64	0.25	0.09
10	1.00	1.00	0.64	1.00	0.64	0.25	0.09
12–20	1.00	1.00	1.00	1.00	0.64	0.25	0.09

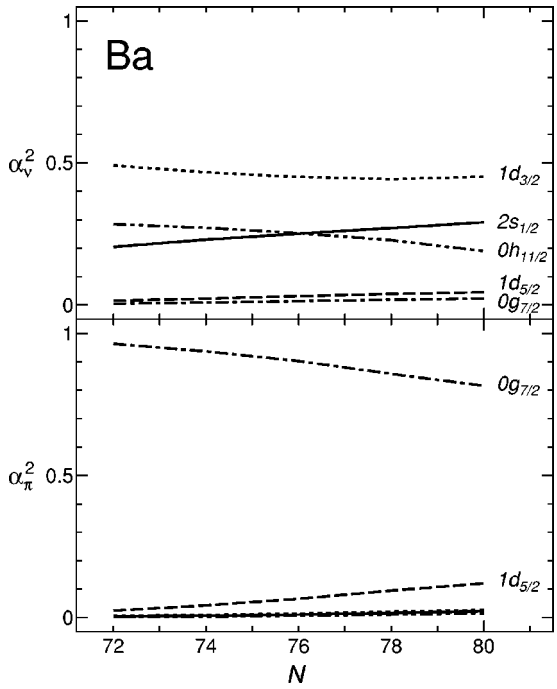

FIG. 1. Structures of S_ν and S_π pairs in terms of valence five orbitals. The sum of all the α's are normalized to 1, i.e., $\Sigma_j \alpha_j^2 = 1$.

Figure 1 shows the structures of S_ν and S_π pairs for Ba isotopes. As seen from the figure the main component of the S_π pair lies in $0g_{7/2}$ orbital while components are spread out mainly in $1d_{3/2}$, $2s_{1/2}$, and $0h_{11/2}$ for the S_ν pair. This can be easily inferred from the adopted single particle energies in Table I. Figure 2 shows the structures of D_ν and D_π pairs, respectively, for Ba isotopes. As seen from the figure the

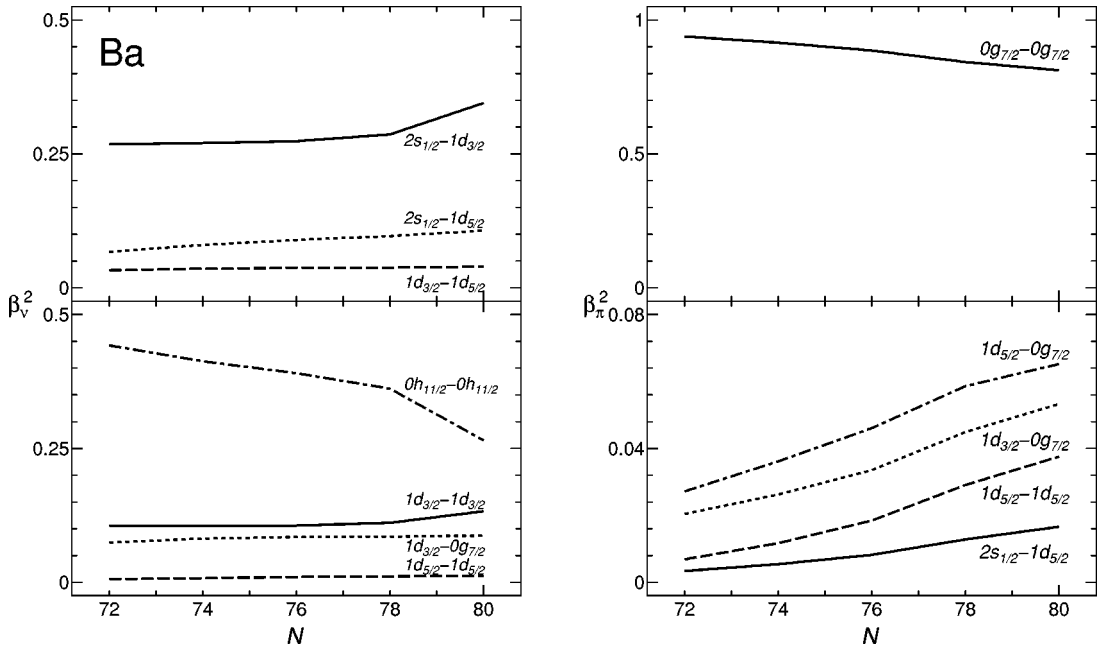

FIG. 2. Structures of D_ν and D_π pairs for Ba isotopes in terms of valence five orbitals. The sum of all the β's are normalized to 1, i.e., $\Sigma_{j_1 \geqslant j_2} \beta^2_{j_1 j_2} = 1$.

main component of the D_π pair is in the $0g_{7/2}$ orbital while components are spread out in $1d_{3/2}$, $2s_{1/2}$, and $0h_{11/2}$ for the D_ν pair.

Figure 3 shows energy spectra of yrast and quasi-γ bands for Xe isotopes. Experimental data are taken from Ref. [41]. We obtain a good agreement with experiment up to spin 6. Energy spectra for Ba isotopes are shown in Fig. 4. We see a better agreement with experiment, compared to Xe isotopes, because quadrupole collectivity becomes more dominant. The experimental energy staggering for the even-spin and odd-spin members of the quasi-γ band, indicating γ instability, is well reproduced except the $N=72$ nucleus, ^{128}Ba. For the $N=80$ nucleus,^{136}Ba, a higher spin pair plays an important role because the quadrupole collectivity is not so dominant near the closed shell.

The spectra for Ce isotopes are shown in Fig. 5, and those for Nd isotopes, in Fig. 6. All four Figs. 3–6 show that theoretical ground- and quasi-γ-band energies smoothly decrease as a function of the number of neutron holes, which well reproduces the experimental behavior except for the $N=72$ isotones. Also the energy-staggering of quasi-γ bands is well reproduced except for the $N=72$ isotones.

The $E2$ transition operator is defined as

$$T(E2;\mu) = e_\nu Q_{\nu\mu} + e_\pi Q_{\pi\mu}, \tag{18}$$

where e_τ ($\tau=\nu$ or π) represents the effective charge of the nucleon, and the operator Q_τ is taken as the quadrupole operator with the oscillator parameter $b=1.005A^{1/6}$ fm . The effective charges are assumed to follow the conventional relation $e_\nu=-\delta e$ and $e_\pi=(1+\delta)e$ [43], and the adopted values are $\delta=0.60+0.05(\overline{N_\nu+N_\pi})$.

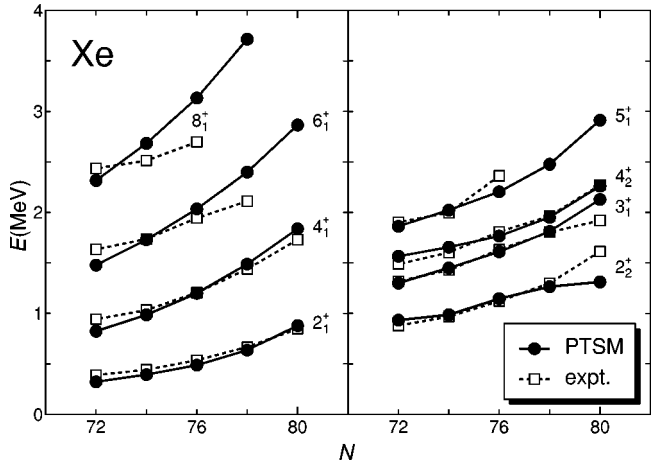

FIG. 3. Energy spectra of the yrast and quasi-γ bands for Xe isotopes as a function of neutron number N.

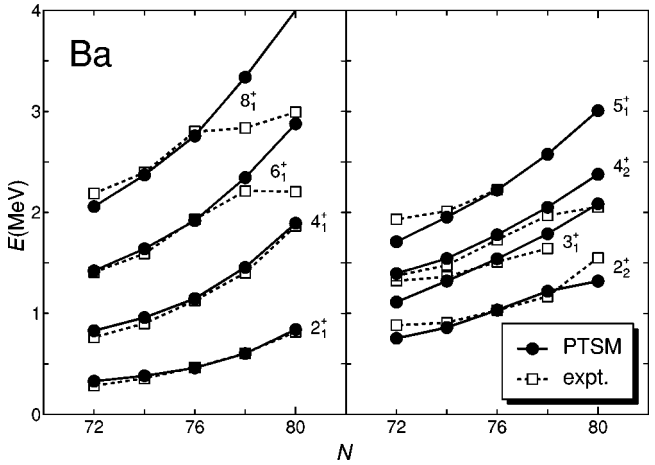

FIG. 4. Energy spectra of the yrast and quasi-γ bands for Ba isotopes.

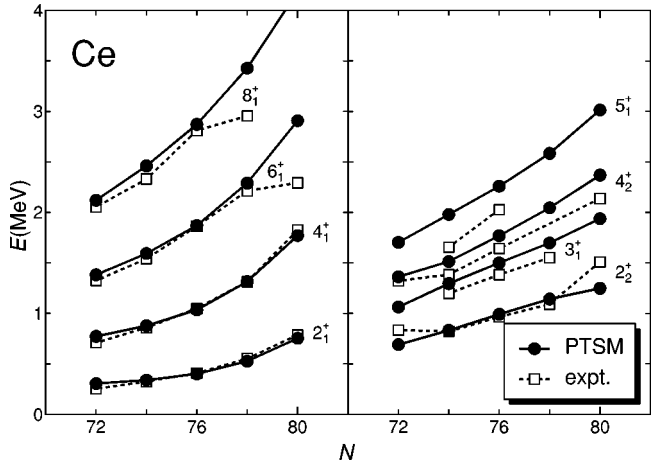

FIG. 5. Energy spectra of the yrast and quasi-γ bands for Ce isotopes.

In Fig. 7 the calculated $B(E2)$ values from the ground state to the first 2^+ state for Xe, Ba, Ce, and Nd isotopes are compared with experiment. Experimental data are taken from Ref. [42]. The overall trend is well reproduced, but we have no good agreement with experiment for $^{132}_{60}\mathrm{Nd}_{72}$. We infer that the calculated deformation is still small compared to the experimental one. After $N=74$ the nuclei rapidly develop deformation, and we may need higher spin pairs such as G pairs to get larger deformation.

Table III shows relative $B(E2)$ values between low-lying states for ^{134}Ba,^{132}Ba, and ^{130}Ba. It is seen that the theoretical results reproduce very well the experimental data, which simulate the O(6) limit prediction of the IBM. In Ref. [13], some $B(E2)$ values were calculated for ^{130}Ba. There they claimed that the $B(E2;0_2^+\rightarrow 2_1^+)$ is equal to $B(E2;0_2^+\rightarrow 2_2^+)$. In our calculation we observe that $B(E2;0_2^+\rightarrow 2_2^+)$ is much smaller than $B(E2;0_2^+\rightarrow 2_1^+)$. This does not mean to deny the statement by Ref. [13] because we observe that these ratios depend largely on the strength of the QP interactions. For instance, in ^{134}Ba, this ratio is almost equal to 1 and there is a large discrepancy between theory and experiment.

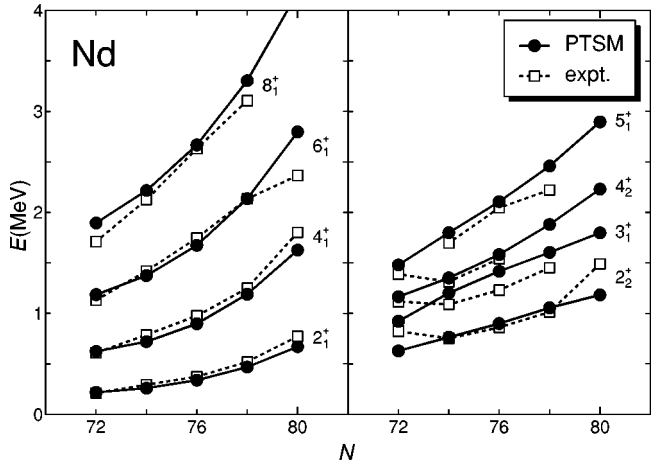

FIG. 6. Energy spectra of the yrast and quasi-γ bands for Nd isotopes.

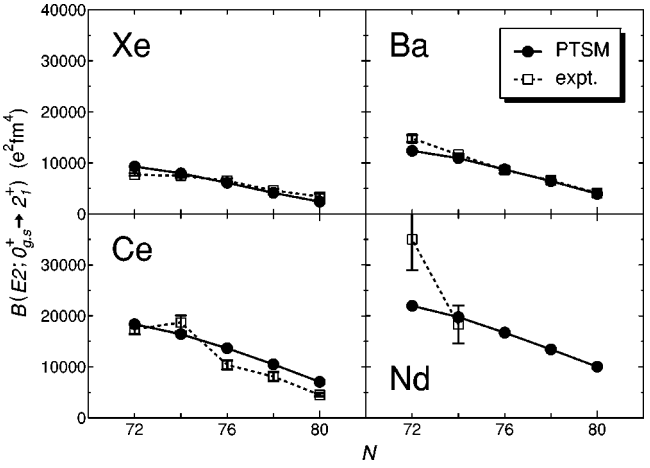

FIG. 7. $B(E2)$ values from the ground state to the first 2^+ state for Xe, Ba, Ce, and Nd isotopes.

B. Odd-mass nuclei

For a description of odd-mass nuclei, we add an unpaired particle to the SD pair core and consider an SD pair plus one-particle state. The state is now written as

$$|jS^{n_s}D^{n_d}J\eta\rangle = [c_j^\dagger|S^{n_s}D^{n_d}J'\eta\rangle]^{(J)}, \tag{19}$$

where J is the total spin, and η an additional quantum number. The number $2n_s+2n_d+1$ represents the total number of valence particles. We use Eq. (17) for the strengths of the interactions.

Figure 8 shows energy levels of odd-mass Xe isotopes. The experimental data are taken from Ref. [41]. Our calculation successfully reproduces the mild change of the ordering of $3/2_1^+$ and $1/2_1^+$ states between the three Xe nuclei. The ordering of $11/2_1^-$ and $9/2_1^-$ is reversely predicted for ^{129}Xe, but fairly well reproduced for ^{131}Xe and ^{133}Xe. Experimentally in ^{133}Xe, $11/2_1^-$ is higher than the ground state $3/2_1^+$, while our model predicts $11/2_1^-$ to be the ground state. For the ordering and position of these negative-parity states we may need an octupole interaction, which is missing in the present calculation. Figure 9 shows energy levels of odd-mass Ba isotopes. Like Xe isotopes, the smooth change of ordering is seen for the $3/2_1^+$ and $1/2_1^+$ states. The ordering of $3/2_2^+$ and $5/2_1^+$ is reversely predicted for ^{133}Ba and ^{135}Ba, but their absolute positions are well reproduced.

Some calculations were also done for Ba and Xe isotopes by the FDSM [16]. In these calculations, energies of positive-parity states were well reproduced, but no energy levels of negative-parity states were given. Figure 10 shows energy levels of odd-mass Ce isotopes. Concerning the first $5/2^+$ state of ^{137}Ce, our calculation seems to fail in reproducing the experimental energy, but theoretically we predict another $5/2^+$ state at around the corresponding energy, and the experimental observation might correspond to this theoretically predicted level. Although reproducing energy levels of odd-mass nuclei is much more difficult compared to even-even nuclei, the agreement is rather well, considering the fact that the effective interactions are solely determined for even-

TABLE III. Comparison of relative $B(E2)$ values between low-lying states for ^{134}Ba,^{132}Ba, and ^{130}Ba. Experimental data are taken from Refs. [44–46].

	^{134}Ba		^{132}Ba		^{130}Ba		O(6)
$J_i^\pi \to J_f^\pi$	PTSM	Expt.	PTSM	Expt.	PTSM	Expt.	
$2_2^+ \to 2_1^+$	100	100	100	100	100	100	100
$\to 0_1^+$	3.3	0.9(2)	<0.01	2.7(4)	0.014	6.2(7)	0
$3_1^+ \to 2_2^+$	100	100	100	100	100	100	100
$\to 4_1^+$	16	⩾2.6	23	38(6)	31	22(3)	40
$\to 2_1^+$	5.1	1.1	1.0	2.6(4)	0.64	4.5(6)	0
$4_2^+ \to 2_2^+$	100	100	100	100	100	100	100
$\to 3_1^+$	7.9		4.2	⩽50(11)	0.36		0
$\to 4_1^+$	22	73	37	73(10)	66	54(10)	91
$\to 2_1^+$	8.4	2.4	4.8	1.8(3)	2.2	2.3(4)	0
$5_1^+ \to 3_1^+$	100	100	100	100	100	100	100
$\to 4_2^+$	60		55	⩽45(7)	48		46
$\to 6_1^+$	10		13		24		45
$\to 4_1^+$	0.053		<0.01	⩽2.2(3)	<0.01		0
$0_2^+ \to 2_2^+$	100	100	100	100	100	100	100
$\to 2_1^+$	107	3.5	9.1	⩽0.7(1)	0.028	3.3(2)	0

even nuclei and no further adjustment is made for odd-mass nuclei.

A lot of information about odd-mass nuclear states is obtained through magnetic moments for which the operator is defined as

$$\boldsymbol{\mu} = \mu_N \sum_{\tau=\nu,\pi} [g_{\ell\tau}\boldsymbol{j}_\tau + (g_{s\tau} - g_{\ell\tau})\boldsymbol{s}_\tau], \tag{20}$$

where $\mu_N(=e\hbar/2mc)$ is the nuclear magneton, and $g_{\ell\tau}(g_{s\tau})$ is the gyromagnetic ratio for orbital angular momentum (spin). The operators $\boldsymbol{j}_\tau$ and $\boldsymbol{s}_\tau$ stand for the angular momentum and spin operators, respectively. The adopted gyromagnetic ratios for orbital angular momentum are $g_{\ell\nu}=0.05$, $g_{\ell\pi}=1.05$, and those for spin are $g_{s\nu}=-2.68$ and $g_{s\pi}=3.91$, which are free nucleon g factors attenuated by a factor of 0.7. These ratios are the same as those in Ref. [22] and the values are fixed through all nuclei concerned in this paper.

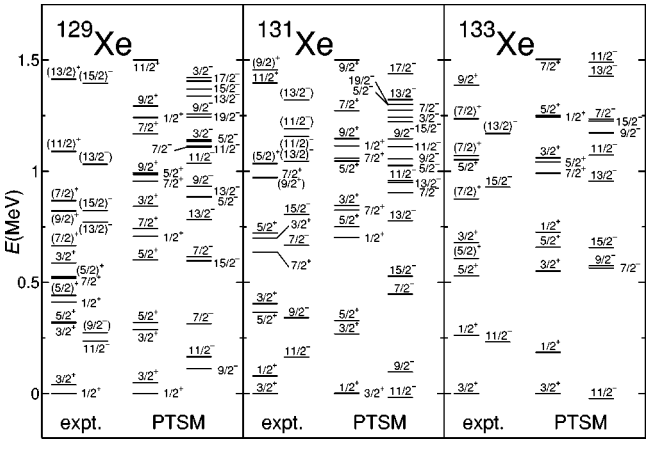

FIG. 8. Comparison of energy spectra of odd-mass Xe isotopes between theory and experiment. Left hand and right hand show experiment (expt.) and theory (PTSM), respectively.

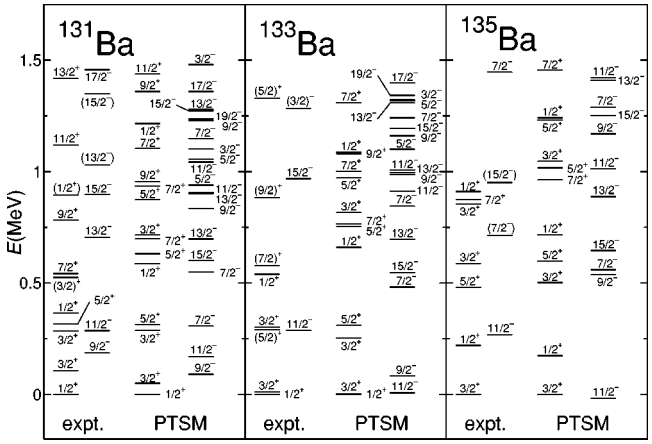

FIG. 9. Comparison of energy spectra of odd-mass Ba isotopes between theory and experiment.

The experimentally known magnetic moments are compared to the calculated values in Table IV. For positive parity states, the magnetic moments are well reproduced except for the $1/2_1^+$ states of ^{129}Xe and ^{131}Ba, which are seven-neutron-hole systems. This might be due to the fact that single-particle levels with positive parity are easily admixed by quadrupole deformation which is expected to be large in seven-neutron-hole systems. The magnetic moments of negative parity states are in excellent agreement with experiment. This clearly shows that negative parity states of even-odd nuclei consist mainly of neutron $0h_{11/2}$ orbital and the neutron spin part largely contributes to the magnetic moments.

IV. SUMMARY AND CONCLUSIONS

Up to now many theoretical investigations have been carried out on even-even nuclei with mass around 130, which exhibit many interesting features coming from the soft triaxial deformation. However, there is a limited number of

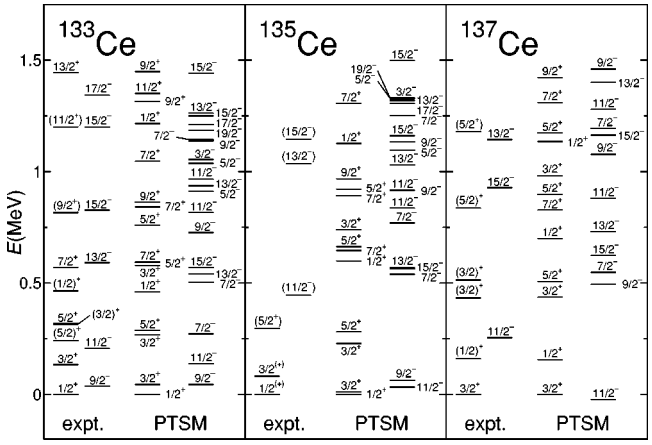

FIG. 10. Comparison of energy spectra of odd-mass Ce isotopes between theory and experiment.

TABLE IV. Comparison of the magnetic moments in the PTSM with experiment (Expt.). The experimental data are taken from Refs. [47–51].

Nucleus	J_i^π	Expt.	PTSM
^{129}Xe	$1/2_1^+$	−0.777976(8)	−0.367
	$3/2_1^+$	+0.58(8)	+0.208
	$11/2_1^-$	−0.8912223(4)	−0.906
^{131}Xe	$3/2_1^+$	+0.6915(2)	+0.515
	$11/2_1^-$	−0.994048(6)	−1.00
^{133}Xe	$3/2_1^+$	+0.81340(7)	+0.868
	$11/2_1^-$	−1.08247(15)	−1.05
^{131}Ba	$1/2_1^+$	−0.709(16)	−0.381
	$9/2_1^-$	−0.870(18)	−0.860
^{133}Ba	$1/2_1^+$	−0.777(14)	−0.625
	$3/2_1^+$	+0.51(7)	+0.514
	$11/2_1^-$	−0.910(51)	−0.972
^{135}Ba	$3/2_1^+$	+0.837943(17)	+0.878
	$11/2_1^-$	−1.001(15)	−1.04
^{137}Ce	$3/2_1^+$	+0.96(4)[a]	+0.918
	$11/2_1^-$	−1.01(4)[a]	−0.996

[a]Only the absolute values are known for the measured magnetic moments of ^{137}Ce.

microscopic researches on odd-mass nuclei due to the difficulty of a theoretical treatment. Here we have proposed the PTSM which can systematically treat even-even and odd-mass nuclei on the equal footing. The PTSM has the feature that the model conserves particle numbers and angular momenta of the states and it is best applied to transitional nuclei. As another aspect, the model has the feature that it drastically and efficiently truncates the gigantic shell model space. For example, the shell model dimension of the 2^+ states in ^{132}Ba amounts to 697 252 966. On the other hand, the number of the corresponding PTSM states reaches only 59.

For even-even nuclei, the subspace of the shell model space is built by the S and D pairs. For a description of odd-mass nuclei, an unpaired neutron is added to the even-even core. As realistic applications of the PTSM to Xe, Ba, Ce, and Nd isotopes, we have used an effective interaction which varies smoothly as a function of neutron and proton numbers. Spectra of both yrast and quasi-γ bands are reproduced very well, along with intraband and interband $B(E2)$ values. We have also applied the same interaction to odd-mass nuclei, and good agreements are obtained for both energy spectra and magnetic moments.

In the present approach we have concentrated on the low-lying states of Xe, Ba, Ce, and Nd isotopes. In order to treat high-spin states including backbending phenomena, we need to extend our model to include high spin pairs coming from $0h_{11/2}$ orbital. For the nucleus ^{132}Ba, such a calculation was already carried out and backbending phenomenon was successfully reproduced [22]. The systematics using high-spin pairs within the framework of the PTSM is now in progress. Another interesting aspect around this region is the controversial argument about the settlement of differences between different IBM approaches, O(6) approach and U(5)-SU(3) one, mentioned in the introduction. Our scheme can provide a microscopic method to answer this question by carrying out a fermion-boson mapping. This will be one of our next important projects.

ACKNOWLEDGMENTS

We would like to thank Professors K. Tanabe, N. Yoshida, A. Gelberg, and Y. M. Zhao for their valuable discussions. One of the authors (K.H.) wishes to acknowledge financial assistance from RIKEN.

[1] J. Yan, O. Vogel, P. von Brentano, and A. Gelberg, Phys. Rev. C **48**, 1046 (1993).
[2] O. Vogel, P. Van Isacker, A. Gelberg, P. von Brentano, and A. Dewald, Phys. Rev. C **53**, 1660 (1996).
[3] F. Iachello and A. Arima, *The Interacting Boson Model* (Cambridge University Press, Cambridge, England, 1987).
[4] S. G. Rohozinski, J. Dobaczewski, B. N. Pomorska, K. Pomorski, and J. Srebrny, Nucl. Phys. **A292**, 66 (1977).
[5] G. Puddu, O. Scholten, and T. Otsuka, Nucl. Phys. **A348**, 109 (1980).
[6] R. F. Casten and P. von Brentano, Phys. Lett. **152B**, 22 (1985).
[7] R. F. Casten, P. von Brentano, K. Heyde, P. Van Isacker, and J. Jolie, Nucl. Phys. **A439**, 289 (1985).
[8] A. Sevrin, K. Heyde, and J. Jolie, Phys. Rev. C **36**, 2631 (1987).
[9] P. von Brentano, A. Gelberg, S. Harissopulos, and R. F. Casten, Phys. Rev. C **38**, 2386 (1988).
[10] X. W. Pan, T. Otsuka, J. Q. Chen, and A. Arima, Phys. Lett. B **287**, 1 (1992).
[11] T. Otsuka, Nucl. Phys. **A557**, 531c (1993).
[12] T. Mizusaki and T. Otsuka, Prog. Theor. Phys. **125**, 97 (1996).
[13] N. V. Zamfir, W.-T. Chou, and R. F. Casten, Phys. Rev. C **57**, 427 (1998).
[14] C. L. Wu, D. H. Feng, X. G. Chen, J. Q. Chen, and M. W. Guidry, Phys. Lett. **168B**, 313 (1986).
[15] C. L. Wu, D. H. Feng, X. G. Chen, J. Q. Chen, and M. W. Guidry, Phys. Rev. C **36**, 1157 (1987).
[16] X. W. Pan, J. L. Ping, D. H. Feng, J. Q. Chen, C. L. Wu, and M. W. Guidry, Phys. Rev. C **53**, 715 (1996).
[17] N. Yoshinaga, Nucl. Phys. **A503**, 65 (1989).
[18] N. Yoshinaga and D. M. Brink, Nucl. Phys. **A515**, 1 (1990).
[19] N. Yoshinaga, Nucl. Phys. **A570**, 421 (1994).
[20] N. Yoshinaga, T. Mizusaki, A. Arima, and Y. D. Devi, Prog. Theor. Phys. **125**, 65 (1996).
[21] N. Yoshinaga, Y. D. Devi, and A. Arima, Phys. Rev. C **62**, 024309 (2000).
[22] K. Higashiyama, N. Yoshinaga, and K. Tanabe, Phys. Rev. C **67**, 044305 (2003).

[23] J. Q. Chen, Nucl. Phys. **A626**, 686 (1997).
[24] Y. A. Luo and J. Q. Chen, Phys. Rev. C **58**, 589 (1998).
[25] Y. M. Zhao, S. Yamaji, N. Yoshinaga, and A. Arima, Phys. Rev. C **62**, 014315 (2000).
[26] Y. A. Luo, J. Q. Chen, and J. P. Draayer, Nucl. Phys. **A669**, 101 (2000).
[27] J. Meyer-Ter-Vehn, Nucl. Phys. **A249**, 141 (1975).
[28] J. Gizon, A. Gizon, and J. Meyer-ter-Vehn, Nucl. Phys. **A227**, 464 (1977).
[29] J. Gizon, A. Gizon, Y. K. Lee, and D. O. Elliott, Phys. Rev. C **17**, 596 (1978).
[30] F. Iachello and P. Van Isacker, *The Interacting Boson-Fermion Model* (Cambridge University Press, Cambridge, England, 1991).
[31] M. A. Cunningham, Nucl. Phys. **A385**, 204 (1982); **A385**, 221 (1982).
[32] H. C. Chiang, S. T. Hsieh, and D. S. Chuu, Phys. Rev. C **39**, 2390 (1989).
[33] S. T. Hsieh, H. C. Chiang, and M. M. King Yen, Phys. Rev. C **41**, 2898 (1990).
[34] D. Bucurescu, G. Cata-Danil, N. V. Zamfir, A. Gizon, and J. Gizon, Phys. Rev. C **43**, 2610 (1991).
[35] J. M. Arias, C. E. Alonso, and R. Bijker, Nucl. Phys. **A445**, 333 (1985).
[36] N. Yoshida, A. Gelberg, T. Otsuka, I. Wiedenhover, H. Sagawa, and P. von Brentano, Nucl. Phys. **A619**, 65 (1997).
[37] C. E. Alonso, J. M. Arias, and M. Lozano, J. Phys. G **13**, 1269 (1987).
[38] B. Fogelberg and J. Blomqvist, Nucl. Phys. **A429**, 205 (1984).
[39] M. Sanchez-Vega, B. Fogelberg, H. Mach, R. B. E. Taylor, A. Lindroth, J. Blomqvist, A. Covello, and A. Gargano, Phys. Rev. C **60**, 024303 (1999).
[40] W. J. Baldridge, Phys. Rev. C **18**, 530 (1978).
[41] NUDAT database, National Nuclear Data Center, http://www.nndc.bnl.gov/nndc/nudat/
[42] S. Raman, C. W. Nestor, Jr., and P. Tikkanen, At. Data Nucl. Data Tables **78**, 1 (2001).
[43] A. Bohr and B. Mottelson, *Nuclear Structure* (Benjamin, New York, 1975), Vol. 1.
[44] A. M. Kleinfeld, A. Bockisch, and K. P. Lieb, Nucl. Phys. **A283**, 526 (1977).
[45] A. Gade, I. Wiedenhover, H. Meise, A. Gelberg, and P. von Brentano, Nucl. Phys. **A697**, 75 (2002).
[46] K. Kirch, G. Siems, M. Eschenauer, A. Gelberg, R. Luhn, A. Mertens, U. Neuneyer, O. Vogel, I. Wiedenhover, P. von Brentano, and T. Otsuka, Nucl. Phys. **A587**, 211 (1995).
[47] M. Kitano, M. Bourzutschky, F. P. Calaprice, J. Clayhold, W. Happer, and M. Musolf, Phys. Rev. C **34**, 1974 (1986).
[48] A. C. Mueller, F. Buchinger, W. Klempt, E. W. Otten, R. Neugart, C. Ekstrom, and J. Heinemeier, Nucl. Phys. **A403**, 234 (1983).
[49] A. I. Grushko, K. E. Kir'yanov, N. M. Miftakhov, Y. P. Smirnov, and V. V. Fedorov, Zh. Eksp. Teor. Fiz. **80**, 120 (1981) [Sov. Phys. JETP **53**, 59 (1981)] .
[50] S. Muto, S. Ohya, K. Heiguchi, and N. Mutsuro, J. Phys. Soc. Jpn. **60**, 845 (1991).
[51] N. J. Stone, Table of Nuclear Magnetic Dipole and Electric Quadrupole Moments, 2001, preprint, Oxford University, United Kingdom, http://www.nndc.bnl.gov/nndc/stone_moments/